# Characteristics of atmospheric pressure rotating gliding arc plasmas

ZHANG Hao (张浩) [1,2], ZHU Fengsen (朱凤森) [1], TU Xin (屠昕) [2]

BO Zheng (薄拯) [1], CEN Kefa (岑可法) [1], LI Xiaodong (李晓东) [1]

[1] State Key Laboratory of Clean Energy Utilization, College of Energy Engineering, Zhejiang University, Hangzhou 310027, China

[2] Department of Electrical Engineering and Electronics, University of Liverpool, Brownlow Hill, Liverpool L69 3GJ, UK

**Abstract**: In this work, a novel direct current (DC) atmospheric pressure rotating gliding arc (RGA) plasma reactor has been developed for plasma-assisted chemical reactions. The influence of gas composition and gas flow rate on the arc dynamic behaviour and the formation of reactive species in the $N_2$ and air gliding arc plasmas has been investigated by means of electrical signals, high speed photography, and optical emission spectroscopic diagnostics. Compared to conventional gliding arc reactors with knife-shaped electrodes which generally require a high flow rate (e.g., 10-20 L/min) to maintain a long arc length and reasonable plasma discharge zone, in this RGA system, a lower gas flow rate (e.g., 2 L/min) can also generate a larger effective plasma reaction zone with a longer arc length for chemical reactions. Two different motion patterns can be clearly observed in the $N_2$ and air RGA plasmas. The time-resolved arc voltage signals show that three different arc dynamic modes, the arc restrike mode, takeover mode, and combined modes, can be clearly identified in the RGA plasmas. The occurrence of different motion and arc dynamic modes is strongly dependent on the composition of working gas and gas flow rate.

**Keywords**: Rotating gliding arc (RGA), gas flow rate, optical emission spectroscopy, motion behavior, electrical characteristics.

**PACS:** 52.30.-q, 52.27.-h, 52.25.-b

## 1. Introduction

Gliding arc discharge (GAD) has been regarded as a promising and efficient technology for

environmental clean-up, energy conversion, and fuel production [1-5]. High reaction rates and fast attainment of steady state in plasma processing allows rapid start-up and shutdown of the processes compared to other thermal treatment processes, which significantly reduces the overall energy cost and offers a promising and flexible route for industrial applications [6-9]. In addition, the electron density ($10^{17}$-$10^{18}$ $cm^{-3}$) of gliding arc plasmas is significantly higher than that of typical non-thermal plasmas (e.g., dielectric barrier discharges and glow discharges), resulting in a better process performance [1,10].

Traditional GAD reactors consist of two divergent knife-shaped electrodes in which the arc initially forms at the narrowest electrode gap and then glides along the electrodes under the force of a gas flow. High flow rate (e.g., 10-20 L/min) is required to push the arc moving along the electrodes, generating a discharge zone for chemical reactions [11,12]. However, not all the reactant gases can pass the plasma zone due to a limited plasma reaction volume confined by the electrodes, which leads to a low retention time of the reactant gases in the plasma zone, and consequently limits the conversions of reactants and energy efficiency of the processes [13,14]. Recent efforts have been placed to the design and development of novel gliding arc systems to enhance the efficiency of plasma chemical processes. Fridman et al. designed a three-dimensional GAD reactor in a reverse vortex flow to generate a transitional plasma that can simultaneously provide a high level of non-equilibrium, high electron temperature, and high electron density [14]. Baba et al. developed a GAD reactor with 3 and 6 electrodes to increase the effective plasma volume for reactions [15]. We have developed a novel DC rotating gliding arc (RGA) reactor co-driven by a magnetic field and tangential flow to generate a stable and thick plasma zone where all the gases can pass through and the arc can rapidly and steadily rotate even at a very low gas flow rate (e.g., 2 L/min). As a result, the retention time of reactant gas flow can be significantly increased. We have shown that this RGA system significantly improves the performance of plasma methane conversion with a maximum $CH_4$ conversion rate of 91.8%, a hydrogen selectivity of 80.7%, and a minimum energy consumption for hydrogen production of 14.3 kJ/L [10].

Although significant efforts have been devoted to investigating the effect of different operating parameters (e.g., input power, flow rate, etc.) on the performance of plasma chemical reactions driven by different gliding arc systems, less attention has been paid to understand the physical

characteristics of these gliding arc plasmas such as the formation of reactive species, arc dynamics, and motion behaviour, which are believed to significantly affect plasma chemical reactions in different ways and could provide valuable information for process optimisation. Therefore, getting new insights into the underlying physical phenomena in the gliding arc plasmas is of primary importance from both scientific and technological points of view.

Gas flow rate has been identified as a key parameter affecting plasma chemical reactions especially in a RGA reactor. In this study, we will investigate the effect of gas flow rate on the spectral characteristics, arc dynamics, and motion behavior of the plasma in a DC RGA reactor operated in $N_2$ and air. $N_2$ and air are selected because they are commonly used as the carrier gases in plasma processes, especially for the decomposition or partial oxidation of hydrocarbons [16-18].

## 2. Experimental

Fig. 1 shows a schematic diagram of the experimental setup. A con-shaped stainless steel electrode (anode) is placed inside a circular cylinder acted as a cathode (stainless steel). Detailed descriptions of the RGA reactor can be found in our previous work [10]. The carrier gas is injected through three tangential inlets at the bottom of the reactor to form a swirling flow in the reactor. A magnet was placed outside the reactor to form a magnetic field for the stabilization and acceleration of the arcs. The arcs move upward and finally rotate rapidly and steadily around position *a* or *b* in the reactor (Fig. 1) with the combined effect of swirling flow and Lorentz force.

The RGA reactor is supplied by a DC power supply (380 V/10 kV) with a 40-kΩ resistance connected in the circuit to limit and stabilize the breakdown current. The electrical signals of the discharges are measured by an oscilloscope (Tektronix DPO4034B) with a high-voltage probe (Tektronix P6015A) and a current probe (Tektronix TCP303). The arc motion behavior is recorded by a high-speed camera (HG-100K with a CMOS sensor). The emission spectra (180-400 nm) of the plasma arcs are recorded by a 750-mm monochromator (PI-Acton 2750, grating: 2400 grooves/mm) equipped with an intensified charge-coupled device (ICCD, PI-MAX 2, 512×512 pixel). An optical fiber is placed at 15 cm above the point *a* to collect the plasma radiation.

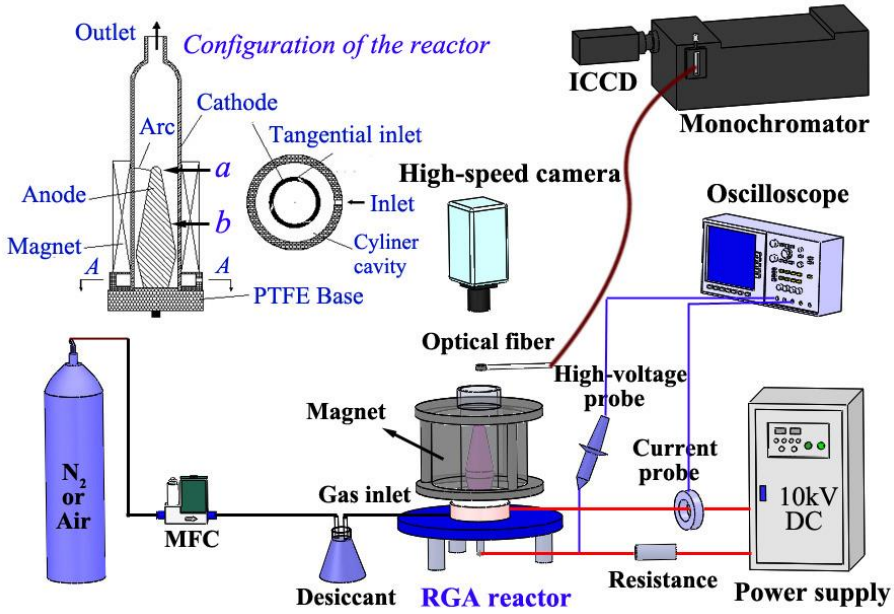


Fig.1 Schematic diagram of the experimental setup

## 3. Results and discussion

### 3.1 Spectral characteristics

Fig. 2 shows the typical emission spectra of the $N_2$ and air RGA plasmas at different gas flow rates. The $N_2$ second positive system (SPS) ($C^3\Pi_u(v') \rightarrow B^3\Pi_g(v'')$, $\Delta v$ = 2, 1, 0, –1, –2, –3) and $N_2^+$ first negative system (FPS) ($B^2\Sigma_u^+(v') \rightarrow X^2\Sigma_g^+(v'')$, $\Delta v$ = 0) are clearly dominated in the spectra of both plasmas. Strong NO γ bands ($A^2\Sigma^+(v') \rightarrow X^2\Pi(v'')$, $\Delta v$ = 1, 0, –1, –2, –3, –4, –5) and weak OH ($A^2\Sigma^+(v') \rightarrow X^2\Pi(v'')$, $\Delta v$ = 0) bands can also be observed in the air plasma. The presence of strong NO γ band indicates the formation of metastable state $N_2$ ($A^3\Sigma_u^+$) in the air plasma since NO ($A^2\Sigma^+$) radicals in the plasma bulk are mainly produced from the reactions of $N_2$ ($A^3\Sigma_u^+$) with NO ($X^2\Pi$) [19]. OH radicals play a key role in many plasma chemical reactions, such as the oxidation of gas and liquid pollutants. In plasma methane reforming processes, OH radicals can react with $CH_4$ to form $CH_x$ (x=1-3) and can also oxidize carbon into CO and $CO_2$ [20]. Interestingly, in both air and $N_2$ gliding arc plasmas, the relative intensity of most molecular bands reaches the peak at the flow rate of 8 L/min and decreases when further increasing the gas flow to 16 L/min.

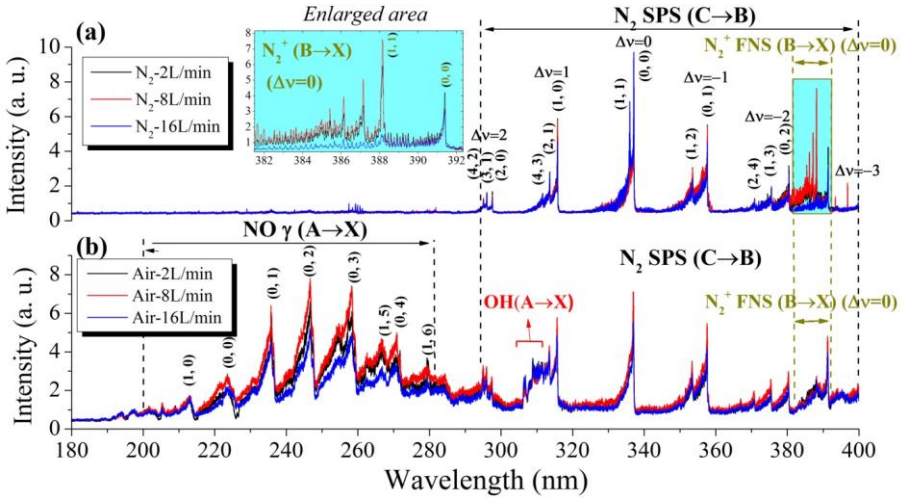


Fig.2 Typical emission spectra of the (a) $N_2$ and (b) air RGA plasmas at different gas flow rates

### 3.2 Motion behavior

Fig. 3 shows the effect of gas flow rate on the motion behavior of the plasma arcs in a rotation cycle. The time interval between two successive arcs in one cycle is 2 ms. The arc was initially formed at the narrowest gap point between the electrodes and then propelled by the swirling flow and Lorentz force to the upper of the inner electrode. Finally, the arc was anchored at the upper point (*a* or *b* as shown in Fig. 1) of the inner electrode and rotated steadily, as shown in Fig. 3. In the $N_2$ RGA at 2 L/min (Fig. 3(a)), the cathode spots move along the inner wall of the outer electrode with a speed of around 8.1 m/s, while the motion velocity of the anode spots is much lower (1.6 m/s).

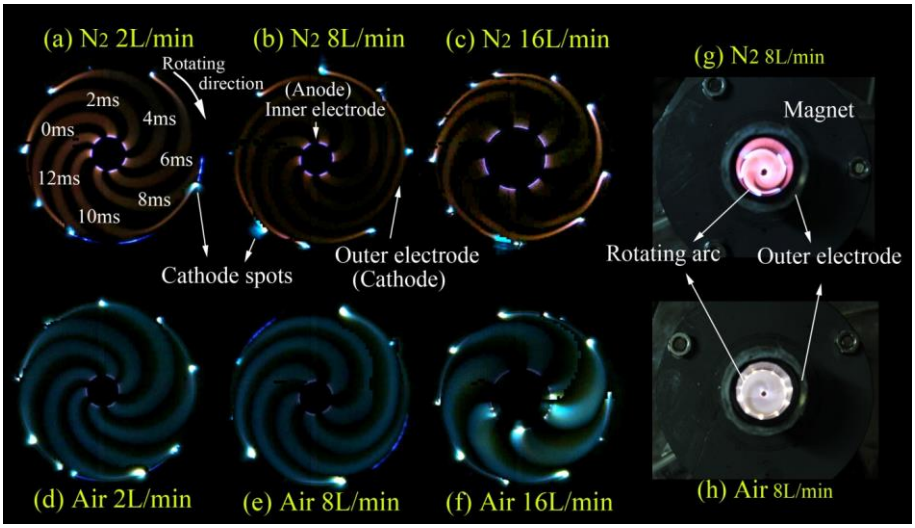


Fig.3 (a)-(f) Composite images of RGA plasmas in a single rotation cycle at different gas flow rates (500 frames/s, exposure time: 997 μs); (g)-(h) photos of the $N_2$ and air RGA plasmas.

Table 1. Motion parameters for the $N_2$ and air RGA plasmas at different gas flow rates

| Parameters \ Flow rate (L/min) | | Pattern A | | Pattern B |
|---|---|---|---|---|
| | | 2 | 8 | 16 |
| Rotation frequency (rps) | $N_2$ | 67 | 78 | 80 |
| | Air | 87 | 111 | 80 |
| Arc length (mm) | $N_2$ | 40.25 | 46.35 | 37.35 |
| | Air | 36 | 38.25 | 31.05 |

The effect of the carrier gas and gas flow rate on the rotation frequency and the assumed arc length was summarized in Table 1. The arc length was calculated as the average length of the arcs in one rotational period. Two motion patterns of the rotating arcs can be identified in the RGA plasmas. Pattern A: at a low gas flow rate (2 or 8 L/min), the rotating arc was finally anchored near the top of the anode (point *a*) with a relative long arc length (40.25-46.35 mm), as shown in Fig. 1. Pattern B: when the gas flow rate further increases to 16 L/min, the rotating arc was finally anchored near point *b* with a shorter arc length (31.05-37.35 mm) compared to the arcs in Pattern A. This could be resulted from the increased turbulence of the plasma arc at a high gas flow rate (e.g., 16 L/min). Similar transition behaviour of the plasma arc was also observed in a DC plasma torch where the plasma arc was transformed from a laminar status to a turbulent flow due to the increase of gas flow rate [21]. It clearly reveals that gas flow rate significantly affects the arc motion behaviour and arc length of the RGA plasmas. In addition, with increasing the flow rate from 2 to 16 L/min, the rotation frequency of the $N_2$ RGA slightly increases from 67 to 80 rotation per second (rps), whereas that of the air RGA reaches a peak of 111 rps at 8 L/min, and then decreases to 80 rps when further increasing the flow rate to 16 L/min.

In a traditional gliding arc reactor with knife-shaped electrodes, a low gas flow causes arc stagnation in the shortest electrode gap. A relatively high flow rate (e.g., 10-20 L/min) is indispensable to enable the arc moving along the electrodes, forming an effective plasma zone for reactions. In addition, only part of the reactant gases can pass through the plasma zone. This leads to a low conversion of reactants in plasma reactions (e.g., methane conversion) due to a significant decrease of the residence time of the reactants in the plasma zone [1]. Interestingly, in this RGA reactor, a relatively low flow rate (e.g., 0.5-2 L/min) can enable arc move to the top of the anode and still maintain a large plasma zone (Pattern A) through the formation of a plasma

"disc", while all the reactant gas flow can pass through the plasma zone, which significantly enhance the performance of plasma chemical reactions [10].

### 3.3 Electrical characteristics

Fig. 4 shows the electrical signals of the $N_2$ and air gliding arc plasmas at different flow rates. Three different arc dynamic modes can be identified, depending on the working gas and gas flow rate. At a flow rate of 8 or 16 L/min with $N_2$ or air as working gas (Fig. 4(b), (c), (e), and (f)), the arc voltage is initially increased slowly, followed by a significant drop (typically a 400 - 600 V drop with a rate of 40 - 60 MV/s) in a very short time (0.8-2.5 ms). The sawtooth waveform of the arc voltage suggests the occurrence of the restrike mode in the RGA plasmas, which can be attributed to the formation of a thick boundary layer between the arc column and the wall of the electrodes [20,22-24]. The presence of the restrike mode in AC traditional gas and gas-liquid gliding arcs with knife-shaped electrodes was also reported [8,20]. In the RGA reactor, a formed arc ($B_1$) is initially elongated by the synergistic effect of swirling flow and Lorentz force, which is reflected by the linear increase of the arc voltage during this period ($B_1$-$A_2$), as shown in Fig. 4(b). When the arc voltage reaches a peak ($A_2$), a breakdown occurs in the boundary layer, forming a new current path and a new arc attachment ($B_2$), which in turn results in a sudden drop of the arc voltage (450 - 550 V drop with a rate of 45 - 50 MV/s). The position of the restrike breakdown on the electrodes is related to the potential distribution in the gas boundary layer between the arc column and electrode wall, which strongly depends on the ionization conditions, thickness, and temperature of the gaseous boundary layer [20]. The arc current varies inversely with the arc voltage and periodic sudden rise of current occurs along with the generation of a new current path.

In the air gliding arc at a flow rate of 2 L/min (Fig. 4(d)), the waveform exhibits a more or less sinusoidal shape. The arc voltage increases and decreases periodically (typically a variation of 420 - 440 V with an increase rate of 56.3 kV/s and a decrease rate of 146.7 kV/s) without a sudden drop of the voltage. The voltage varies with a relatively regular period of around 11 ms. The arc dynamic behaviour can be characterized as a typical takeover mode. In this mode, the electric field intensity is not high enough to lead to a breakdown at the gas boundary layer. So the cathode spots move smoothly along the inner wall of the cathode without restrike. The regular

and smooth increase and decrease of the arc voltage reflect the elongation and contraction of the arc in the motion of arc spots.

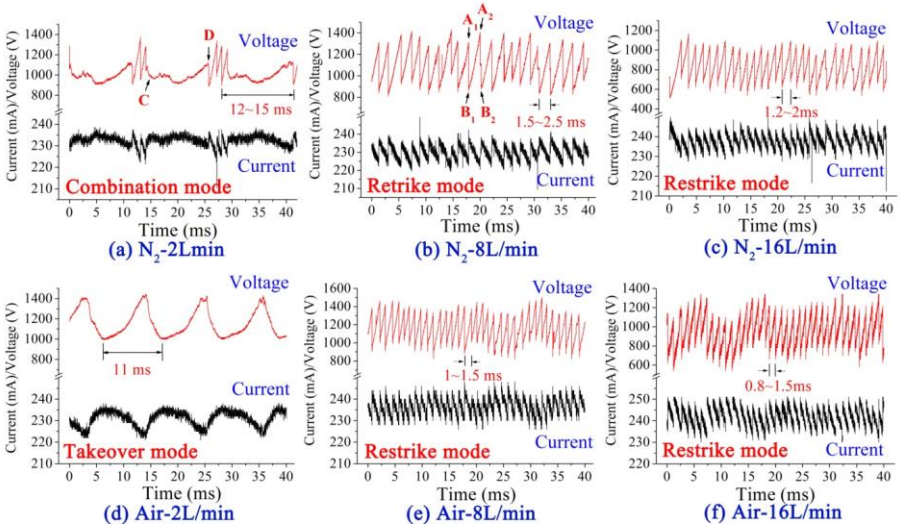


Fig.4 Electrical signals of the $N_2$ and air RGA plasmas at different gas flow rates

In the $N_2$ gliding arc at a flow rate of 2 L/min (Fig. 4(a)), we find a weak variation of the arc voltage followed by one or more sudden voltage drops, while the period of the waveforms is 12~15 ms, showing a combination of the restrike and takeover modes. As shown in Fig. 4(a), a new current path (C) will last for 12~15 ms. During this period (C-D), the change of the arc length accounts for the variation of the arc voltage and current. Then, the restrike of the arc (D) occurs for one or several times. The combined restrike and takeover dynamic behaviour can also be observed in DC arc plasma torches [25].

## 4. Conclusion

The physical characteristics of the DC $N_2$ and air rotating gliding arc plasmas have been investigated by using a high-speed camera, optical emission spectroscopic diagnostics, and electrical signal analysis. A plasma “disc” is generated through rapid and steady rotation of the arcs between the electrodes with a rotation frequency of 67-111 rps around the inner electrode. Two motion patterns of the $N_2$ and air plasma arcs could be observed. At a low gas flow rate of 2 and 8 L/min, the arc is anchored near the top of the anode (point *a*) with a much longer arc length, while further increasing the gas flow to 16 L/min leads to the shortening of the arc with finally

anchored at point *b*. In addition, three different arc dynamic modes, the restrike mode, takeover mode, and combined modes can be clearly identified. They are totally dependent on the gas composition and gas flow rate.

**Acknowledgments**

Supported of this work by the Specialized Research Fund for the Doctoral Program of Higher Education of China (No. 20120101110099) and the Fundamental Research Funds for the Central Universities (No. 2014FZA4011) is gratefully acknowledged.

**References**

1 Tu X, Whitehead J C. 2014, International Journal of Hydrogen Energy, 39: 9658.

2 Tu X, Yu L, Yan J H, et al. 2010, IEEE Transactions on Plasma Science, 38: 3319.

3 Ni Mingjiang, Yang H, Chen T, et al. 2015, Plasma Science and Technology, 17: 209.

4 Li X D, Zhang H, Yan S X, et al. 2013, IEEE Transactions on Plasma Science, 41: 126.

5 Gutsol A, Rabinovich A, Fridman A. 2011, Journal of Physics D: Applied Physics, 44: 274001.

6 Petitpas G, Rollier J, Darmon A, et al. 2007, International Journal of Hydrogen Energy, 32: 2848.

7 Zhang H, Li X D, Zhang Y Q, et al. 2012, IEEE Transactions on Plasma Science, 40: 3493.

8 Tu X, Gallon H J, Whitehead J C. 2011, IEEE Transactions on Plasma Science, 39: 2900.

9 Zhang C, Shao T, Xu J, et al. 2012, IEEE Transactions on Plasma Science, 40: 2843.

10 Zhang H, Du C M, Wu A J, et al. 2014, International Journal of Hydrogen Energy, 39: 12620.

11 Feng Z, Saeki N, Kuroki T, et al. 2012, Applied Physics Letters, 101: 41602.

12 Zhu J, Gao J, Li Z, et al. 2014, Applied Physics Letters, 105: 234102.

13 Lee D H, Kim K T, Cha M S et al. 2007, Proceedings of the Combustion Institute, 31: 3343.

14 Kalra C S, Cho Y I, Gutsol A, et al. 2005, Review of Scientific Instruments, 71: 25110.

15 Baba T, Takeuchi Y, Stryczewska H D et al. 2012, Przegląd Elektrotechniczny, 88: 86.

16 Shao T, Tarasenko V F, Yang W, et al. 2014, Plasma Sources Science and Technology, 23: 54018.

17 Shao T, Zhang C, Niu Z, et al. 2011, Applied Physics Letters, 98: 21503.

18 Tu X, Whitehead J C. 2012, Applied Catalysis B: Environmental, 125: 439.

19 Panousis E, Panousis E, Spyrou N, et al. 2009, IEEE Transactions on Plasma Science, 33: 1004.

20 Tu X, Yu L, Yan J H, et al. 2009, Physics of Plasmas, 16: 113506.

21 Pan Wenxia, Xian Meng, Wu Chengkang. 2006, Plasma Science and Technology, 8: 416.

22 Eckert E, Pfender E, Wutzke S A. 1967, Aiaa Journal, 5: 707.

23 Moreau E, Chazelas C, Mariaux G, et al. 2006, Journal of Thermal Spray Technology, 15: 524.

24 Tu X, Yan J H, Yu L, et al. 2007, Applied Physics Letters, 91: 131501.

25 Dorier J L, Gindrat M, Hollenstein C, et al. 2001, IEEE Transactions on Plasma Science, 29: 494.

E-mail addresses of TU Xin and LI Xiaodong: xin.tu@liv.ac.uk and lixd@zju.edu.cn